Eur. Phys. J. E (2017) **40**: 92
DOI 10.1140/epje/i2017-11582-8

THE EUROPEAN PHYSICAL JOURNAL E

Regular Article

Viscous dissipation and dynamics of defects in an active nematic interface*

Len M. Pismen[1,a] and Francesc Sagués[2]

[1] Department of Chemical Engineering, Technion – Israel Institute of Technology, 32000 Haifa, Israel
[2] Departament of Materials Science and Physical Chemistry, Institut de Nanociència i Nanotecnologia, Universitat de Barcelona, Martí Franquès 1, 08028 Barcelona, Spain

Received 25 July 2017 and Received in final form 24 August 2017
Published online: 26 October 2017 –

Abstract. We consider active flow and dynamics of topological defects in an active nematic interfacial layer confined between immissible viscous fluid layers. The velocity of defects is determined by asymptotic matching of solutions in the defect core and the far field. Self-propulsion of positive defects along the direction of their "comet tails" is identified as the principal deterministic component of defect dynamics, while topological and hydrodynamic interactions among mobile defects is responsible for quasi-random jitter.

1 Introduction

Soft active matter has emerged during the last decade as a new paradigm in the field of non-equilibrium condensed-matter physics [1,2]. Living realisations, from animal flocks [3] to bacterial colonies [4,5] or cytoskeletal components [6–8], as well as non-living replicas, composed of either externally driven [9–11] or autonomously propelled elements [12–14], share a common distinctive feature: elementary units convert ambient or stored energy into large-scale clusters and flows, from coherently organised to seemingly chaotic.

Cytoskeletal reconstitutions, based on the entanglement of filamentary and motor proteins, are singularly motivating for their biophysics interest. Particularising to extensile systems, we will focus on the system pioneered by the group of Dogic [8], based on the hierarchical self-assembly of tubulin, all the way up from monomers to micron-size stabilised microtubules (MTs). The latter are forced to bundle by the action of a depleting passive (non-adsorbing) polyethylene-glycol (PEG) agent, while they are internally cross-linked and sheared by clusters of ATP-fueled kinesin motors. Inter-filament sliding occurs in bundles containing MTs of opposite polarity. In volume prepared samples this mixture self-organises into an active gel continuously reconstituted following bundle reorganisation [8,15]. Alternative preparations of this lyotropic-like system appear as bundled MTs two-dimensionally assembled either at planar [8,16,17] or curved [18] interfaces. In both cases, one observes textures characteristic of a 2D-nematic, that are punctuated by half-integer defects (fig. 1) and permeated by streaming flows.

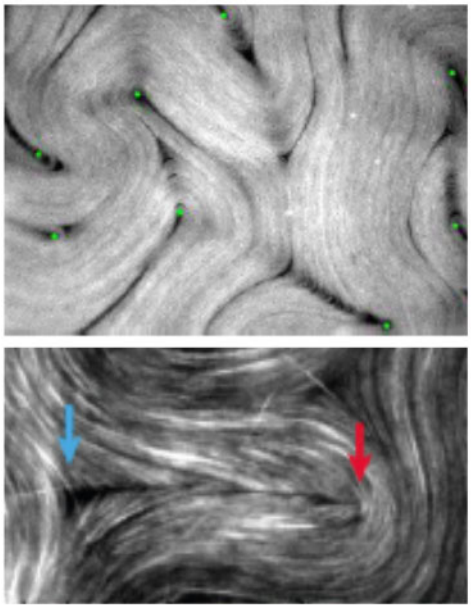

Fig. 1. Above: a typical texture of an active nematic layer [17]. Points indicate locations of $+1/2$ defects. Below: close-up on paired $+1/2$ and $-1/2$ defects (indicated by arrows).

Topological defects commonly arise in liquid-crystalline media following transition from the isotropic

* Contribution to the Topical Issue "Non-equilibrium processes in multicomponent and multiphase media" edited by Tatyana Lyubimova, Valentina Shevtsova and Fabrizio Croccolo.

[a] e-mail: pismen@techunix.technion.ac.il

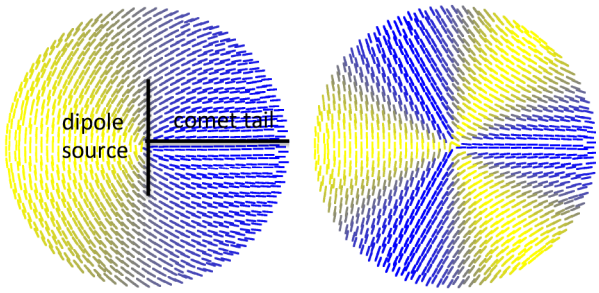

Fig. 2. The core structure of $+1/2$ (left) and $-1/2$ (right) defects. Dashes indicate the director orientation, and shading imitates patterns observed using the Schlieren technique. The left picture shows the direction of the "comet tail", further taken as the x-axis and the origin of the polar angle, and the orientation of the dipolar vorticity source (see sect. 3.2).

state, as a result of different ordering in spatially removed domains [19,20]. In thin nematic layers with in-plane director orientation, defects with the lowest energy have charge $\pm 1/2$. The core structure of these defects is sketched in fig. 2, showing their distinct symmetries. In common passive nematics, defects gradually annihilate, leading eventually to a monodomain state or, depending on boundary conditions, to a texture with the minimal number of defects. This evolution is accompanied by flow that ceases when the final lowest-energy state is attained. In contrast to this, in active nematics defects may arise spontaneously due to an instability of a perfectly aligned state [21]. Equilibrium is never reached, and the motion of defects due to their topological attraction is complemented by spontaneous motion driven by the active stress that originates, in the experimental system under the discussion, in the action of ATP-fueled kinesin motors.

We will restrict our attention to such 2D active dynamics but stressing its interfacial aspects when facing other passive soft-matter components [16,17] where an ultrathin active layer plays a role of a surfactant localised on the oil-water interface. In fact, the possibility of interfacial active materials makes them a lot more attractive from the point of view of both biophysics and material science. Theoretical and numerical studies were mostly restricted so far to thin active nematic layers lacking such kind of contact with passive soft media, and therefore inapplicable to the experiments of this kind. Simulations of flow and nematic textures in active layers [22,23] were based on solving the 2D Navier-Stokes equation, which, if applied to a thin layer, presumes perfect slip at the confining planes. In the free-slip 2D setting, the momentum transfer from active medium is impeded, leading to far-field divergences mitigated by inertial screening, which leads to an $O(1)$ Reynolds number based on the correlation length [23]. With a different perspective from the lubrication ansatz employed here, an attempt to incorporate hydrodynamic coupling has been published very recently to try to estimate the shear viscosity of an active nematic film from experiments with an open cell [17]. On the other hand, the analytical study of defect dynamics by one of the authors [21] used the lubrication approximation to describe a more realistic no-slip Hele-Show geometry with strong wall friction. In what follows, we adjust this technique to experiments performed with the tubulin/kinesin active nematic bound to an oil-water interface in a closed flow cell. We aim at analysing the response of the active material to this particular interfacial rheological condition, looking mostly at the most significant features of the active nematic, *i.e.* the proliferation of defects and the associated streaming currents.

2 Nematic texture

We consider an ultrathin flat layer of active nematic confined between two fluid layers. The analysis largely follows earlier theory [21], where, however, a thin active layer was assumed to be confined between solid walls. The nematic order parameter in the active layer depends on in-plane coordinates $\mathbf{r} = (x, y)$, and 2D formulation is applicable. The 2D nematic order parameter is a traceless symmetric tensor with the components $Q_{ij} = \rho(2n_i n_j - \delta_{ij})$, where ρ is its absolute value, $\mathbf{n} = (\cos\theta, \sin\theta)$ is the unit director, θ is the orientation angle, and δ_{ij} is the Kronecker delta. An equivalent more convenient representation is

$$\mathbf{Q} = \begin{pmatrix} p & q \\ q & -p \end{pmatrix} \equiv \rho \begin{pmatrix} \cos 2\theta & \sin 2\theta \\ \sin 2\theta & -\cos 2\theta \end{pmatrix}, \qquad (1)$$

with $\rho = (p^2 + q^2)^{1/2}$. The nematic energy per unit thickness is expressed as $\mathcal{F} = \int \mathcal{L}\, \mathrm{d}^2\mathbf{r}$ with the 2D Landau-de Gennes Lagrangian [19]

$$\mathcal{L} = -\frac{\alpha}{4} Q_{ij}Q_{ij} + \frac{\alpha}{16}\left(Q_{ij}Q_{ij}\right)^2 + \frac{\kappa_1}{2}\left|\partial_i Q_{ij}\right|^2 + \frac{\kappa_2}{4}\sum_{ijk}\left(\partial_i Q_{jk}\right)^2. \qquad (2)$$

The coefficients at the algebraic terms are rescaled to the common value α to ensure $\rho = 1$ in the homogeneous nematic state; the cubic term vanishes identically in 2D. The number of distinct elastic constants κ_1, κ_2 reduces to two when their anisotropy is neglected, similar to the one-constant approximation in the case $\rho = 1$. The Lagrangian can be rewritten in terms of p and q as

$$\mathcal{L} = -\frac{\alpha}{2}\left(q^2 + p^2\right) + \frac{\alpha}{4}\left(q^2 + p^2\right)^2 + \frac{\kappa_1}{2}\left[(p_x + q_y)^2 + (q_x - p_y)^2\right] + \frac{\kappa_2}{2}\left[p_x^2 + p_y^2 + q_x^2 + q_y^2\right]. \qquad (3)$$

Relaxation to equilibrium follows the gradient dynamics governed by the variational equation of the form $\partial_t \mathbf{Q} = -\Gamma \delta\mathcal{F}/\delta\mathbf{Q}$ with the mobility coefficient Γ. Scaling time t by $(\alpha\Gamma)^{-1}$ and length by the healing length $\xi = \sqrt{(\kappa_1 + \kappa_2)/\alpha}$, and varying eq. (3) yields the dynamic equations in a particularly simple form:

$$p_t = \nabla^2 p + p - (p^2 + q^2)p, \qquad q_t = \nabla^2 q + q - (p^2 + q^2)q, \quad (4)$$

where ∇^2 is the 2D Laplacian. These equations reduce to a single equation for the complex variable $\chi = p + \mathrm{i}\, q = \rho \mathrm{e}^{\mathrm{i}\,\vartheta}$ identical to the equation of dissipative dynamics of a vortex of unit charge in a complex scalar field [20]:

$$\chi_t = \nabla^2\chi + \chi - |\chi|^2\chi. \tag{5}$$

In a planar film flowing or deforming with the velocity $\mathbf{u}$ and vorticity $\omega = \nabla \times \mathbf{u}$, the time derivative should be replaced by the corotational substantial derivative

$$\mathcal{D}_{ijkl}Q_{kl} = (\partial_t + \mathbf{u}\cdot\nabla)Q_{ij} + \frac{\omega}{2}(\epsilon_{li}Q_{kj} - \epsilon_{ik}Q_{lj}), \tag{6}$$

where ϵ_{ki} is the antisymmetric tensor. This brings eqs. (4), (5) to the form

$$p_t + \mathbf{u}\cdot\nabla p + \omega q = \nabla^2 p + p\left(1 - p^2 - q^2\right), \tag{7}$$

$$q_t + \mathbf{u}\cdot\nabla q + \omega p = \nabla^2 q + q(1 - p^2 - q^2), \tag{8}$$

$$\chi_t + \mathbf{u}\cdot\nabla\chi + \mathrm{i}\,\omega\chi = \nabla^2\chi + \chi - |\chi|^2\chi. \tag{9}$$

Consider a static defect with the charge $\pm\frac{1}{2}$. In its far field, *i.e.* at distances from the core exceeding the healing length (taken here as unity), $\rho \to 1$ and $\vartheta = 2\theta = \pm\phi$, where ϕ is the polar angle. The solution in the defect core can be obtained using the *ansatz* $\chi = \rho(r)\mathrm{e}^{\pm\mathrm{i}\,\phi}$, leading to the equation defining the dependence of the scalar order parameter $\rho = |\chi|$ on the radial coordinate r:

$$\rho_{rr} + r^{-1}\rho_r - r^{-2}\rho + (1 - \rho^2)\rho = 0. \tag{10}$$

This defines the well-known short-scale core structure $\rho(r)$, identical to that of a superfluid vortex of unit charge. The asymptotics of this solution are $\rho \approx ar$ at $r \to 0$, where the constant a is computed numerically as $a \approx 0.583$, and $\rho(r) \asymp 1 - \frac{1}{2}r^{-2}$ at $r \gg 1$. A useful analytical form of $\rho(r)$ is a Padé approximant [20] with the same leading-order asymptotics at both zero and infinity, that fairly approximates the numerical solution in the entire domain:

$$\rho(r) = r\sqrt{\frac{0.34 + 0.07r^2}{1 + 0.41r^2 + 0.07r^4}}\,. \tag{11}$$

3 Flow induced by defects

3.1 Basic equations

We will now explore both active and passive flow induced by defects in the nematic layer and in the isotropic passive fluids layers bounding it from above and below. The latter are described in the lubrication approximation reducing the Stokes equation for the horizontal velocities $\mathbf{u}_\pm$ to $\eta_\pm\mathbf{u}_\pm''(z) = \nabla P$, where the pressure P is constant across both upper (marked by the plus sign) and lower (marked by the minus sign) layers, $\eta_\pm$ are the respective viscosities, and ∇ is the 2D gradient operator. Taking the active layer as the plane $z = 0$, we impose the no-slip boundary conditions at $z = \pm h_\pm$ and the continuity condition at $z = 0$:

$$\mathbf{u}_\pm(0) = \mathbf{u}, \qquad \mathbf{u}_\pm(-h_\pm) = 0, \tag{12}$$

where $\mathbf{u}$ is the velocity in the active layer. This leads to the velocity profiles

$$\mathbf{u}_\pm = \mathbf{u} + b_\pm z + \frac{\nabla P}{2\eta_\pm}z^2, \quad b_\pm = \frac{\nabla P}{2\eta_\pm}h_\pm + \frac{\mathbf{u}}{h_\pm}\,. \tag{13}$$

The flow field $\mathbf{u}(\mathbf{r}, z)$ in the active layer is determined by the generalised 2D Stokes equation complemented by the terms expressing the friction with the bounding passive layers:

$$\eta\nabla^2\mathbf{u} - (\eta_+ b_+ + \eta_- b_-) = \nabla P - \nabla\cdot\left(\boldsymbol{\sigma}^{(\mathrm{a})} + \boldsymbol{\sigma}^{(\mathrm{p})}\right), \tag{14}$$

where η is the 2D viscosity of the active layer (with the viscous anisotropy neglected), $\boldsymbol{\sigma}^{(\mathrm{a})} = \zeta\alpha\mathbf{Q}$ is the active stress [24] with the activity parameter ζ, and $\boldsymbol{\sigma}^{(\mathrm{p})} = -\partial_j Q_{kl}\partial\mathcal{L}/\partial(\partial_i Q_{kl})$ is the passive Ericksen stress.

Taking the curl of eq. (14) to eliminate pressure yields the equation of vorticity $\omega(\mathbf{r})$. We write it in the dimensionless form, scaling velocity by $\xi/(\Gamma\alpha)$, and stress by α:

$$\nabla^2\omega - \beta\omega = \Phi, \quad \Phi = \varepsilon\nabla\times\left[\nabla\cdot\left(\boldsymbol{\sigma}^{(\mathrm{a})} + \boldsymbol{\sigma}^{(\mathrm{p})}\right)\right]. \tag{15}$$

The dimensionless parameters of the problem are

$$\varepsilon = \frac{\zeta}{\eta\Gamma}, \qquad \beta = \frac{\xi^2}{\eta}\left(\frac{\eta_+}{h_+} + \frac{\eta_-}{h_-}\right). \tag{16}$$

The former can be viewed as the ratio of the characteristic elastic-to-viscous relaxation times in the active layer, and the latter is the effective friction coefficient. Since $\xi \ll h_\pm$, the lubrication approximation for the passive layers breaks down near the defect location but viscous dissipation in the active layer prevails there over friction in the realistic case $\beta \ll 1$.

3.2 Active flow

We compute first the contribution of the active stress generated by a defect placed at the origin of the polar coordinate system $\{r, \phi\}$. Taking $\boldsymbol{\sigma} = \boldsymbol{\sigma}^{(\mathrm{a})} = \zeta\mathbf{Q}$, we express the inhomogeneity in eq. (15) for defects with the charge $\pm\frac{1}{2}$ as

$$\begin{aligned}\Phi_+^{(\mathrm{a})} &= -\varepsilon\sin\phi\left(\rho_{rr} + r^{-1}\rho_r - r^{-2}\rho\right)\\ &= \varepsilon\rho(1 - \rho^2)\sin\phi,\\ \Phi_-^{(\mathrm{a})} &= -\varepsilon\sin 3\phi\left(\rho_{rr} - 3r^{-1}\rho_r + 3r^{-2}\rho\right),\end{aligned} \tag{17}$$

where the last expression for $\Phi_+^{(\mathrm{a})}$ is written using eq. (10). In a positive defect, activity generates within the defect core a force oriented along the "comet tail", leading to a normally oriented dipolar vorticity source (see fig. 2). A negative defect has a different structure with the threefold symmetry, and a sextuplet vorticity source is generated instead. The vorticity due to a positive defect can be presented as $\omega_+^{(\mathrm{a})} = -\varepsilon\upsilon(r)\sin\phi$, where $\upsilon(r)$ satisfies

$$\upsilon_{rr} + r^{-1}\upsilon_r - (\beta + r^{-2})\upsilon + (1 - \rho^2)\rho = 0. \tag{18}$$

After solving this equation with the boundary conditions $v(0) = v(\infty) = 0$, one can compute the stream function with the same symmetry $\Psi = \varepsilon\psi(r)\sin\phi$ satisfying $\nabla^2\Psi = \omega$, or equivalently

$$\psi_{rr} + r^{-1}\psi_r - r^{-2}\psi + v(r) = 0. \tag{19}$$

This corresponds to the flow field

$$\mathbf{u}_+^{(a)} = \nabla\times\Psi = \varepsilon\left\{\begin{array}{c} r^{-1}\psi\cos^2\phi + \psi_r\sin^2\phi \\ \frac{1}{2}\sin 2\phi(r^{-1}\psi - \psi_r)\end{array}\right\}. \tag{20}$$

For a negative defect, we write in a similar way $\omega_-^{(\mathrm{a})} = -\varepsilon v(r)\sin 3\phi$, where $v(r)$ satisfies

$$v_{rr}+r^{-1}v_r-(\beta+9r^{-2})v-\rho_{rr}+3r^{-1}\rho_r-3r^{-2}\rho = 0. \tag{21}$$

The respective stream function is $\Psi = \varepsilon\psi(r)\sin 3\phi$, where $\psi(r)$ satisfies

$$\psi_{rr} + r^{-1}\psi_r - 9r^{-2}\psi + v(r) = 0. \tag{22}$$

This corresponds to the flow field

$$\mathbf{u}_-^{(a)} = \varepsilon\left[\frac{3}{2}\frac{\psi}{r}\left\{\begin{array}{c}\cos 2\phi + \cos 4\phi \\ \sin 2\phi(2\cos 2\phi - 1)\end{array}\right\} + \frac{1}{2}\psi_r\left\{\begin{array}{c}\cos 2\phi - \cos 4\phi \\ -\sin 2\phi(2\cos 2\phi + 1)\end{array}\right\}\right]. \tag{23}$$

As before, vorticity decays asymptotically as r^{-2}, and the far-field asymptotics of the flow field is

$$\mathbf{u}_-^{(a)} \asymp \frac{1}{12}\frac{\varepsilon}{\beta r}\left\{\begin{array}{c}\cos 2\phi + \cos 4\phi \\ \sin 2\phi(2\cos 2\phi - 1)\end{array}\right\}. \tag{24}$$

The total active flow field is a superposition of flow induced by all extant defects but this simple superposition breaks down near defect cores.

3.3 Passive flow

The passive Ericksen stress is expressed in the adopted units as

$$\sigma_{ij}^{(\mathrm{p})} = -2(\varepsilon/\zeta)\left(\partial_i p\partial_j p + \partial_i q\partial_j q + \kappa_1\xi^{-2}\delta_{ij}\epsilon_{kl}\partial_k p\partial_l q\right), \tag{25}$$

where δ_{ij} is the Kronecker delta and ϵ_{kl} is the 2D antisymmetric matrix. Only the first term contributes to the inhomogeneity in eq. (15), which is expressed as $\Phi^{(\mathrm{p})}(r,\phi) = \mp 2\varepsilon\sin 2\phi f_{\mathrm{p}}(r)$ with

$$f_{\mathrm{p}}(r) = \rho_{rr}^2 + \rho_r\rho_{rrr} - r^{-2}\rho_r^2 - r^{-3}\rho\rho_r + r^{-4}\rho^2. \tag{26}$$

This reduces to $\Phi^{(\mathrm{p})}(r) = \mp 2r^{-4}\sin 2\phi$ in the far field. The far-field vorticity solving eq. (15) decays asymptotically as r^{-4}, which corresponds to a quadrupole flow field decaying as r^{-3} at $r\to\infty$. Due to the faster decay, the passive stress can be dissipated in the nematic layer, without a necessity to transfer the momentum to solid walls indispensable for the active stress. The exact expression for the flow field, obtained by computing as above the vorticity and the stream function $\Psi = \psi(r)\sin 2\phi$, has the form

$$\mathbf{u}^{(p)} = \frac{\varepsilon}{\zeta}\left\{\begin{array}{c}\cos\phi(r^{-1}\psi\cos 2\phi + \psi_r\sin^2\phi) \\ \sin\phi(r^{-1}\psi\cos 2\phi + \psi_r\cos^2\phi)\end{array}\right\}. \tag{27}$$

4 Perturbed defect core

4.1 Solvability condition

The defect velocity under the combined action of orientation gradients and flow induced by other defects, as well as self-induced active flow, is computed by asymptotic perturbation analysis assuming that the defect core structure is only weakly perturbed. Assuming that the defect motion is quasistationary, it is advantageous to transform eq. (9) to the frame comoving and corotating with the defect: $\chi_t \to \widetilde{\mathbf{U}}\cdot\nabla\chi + \mathrm{i}\,\widetilde{\Omega}\chi$, where $\widetilde{\mathbf{U}}$, $\widetilde{\Omega}$ are, respectively, the translational and rotational velocities of the defect relative to the surrounding active fluid, so far unknown. Note that rotation is a non-trivial effect, since the orientation field around the defect lacks circular symmetry. The flow velocity induced by other defects, removed at a distance R large compared with the core size, is constant across the core in the leading order in $1/R$. Therefore it does not perturb the core structure, and can be eliminated by the transformation to the comoving frame, so that $\widetilde{\mathbf{U}}$, $\widetilde{\Omega}$ are replaced by absolute translational and rotational velocities of the defect $\mathbf{U}$, Ω. The remaining variable advective term contains the self-induced velocity $\mathbf{u} = \mathbf{u}_+^{(a)} + \mathbf{u}_-^{(a)} + \mathbf{u}_+^{(p)}$. Thus, eq. (9) is reduced to the form

$$(\mathbf{U}+\mathbf{u})\cdot\nabla\chi + \mathrm{i}\,(\Omega+\omega)\chi = \nabla^2\chi + \chi(1-|\chi|^2) = 0. \tag{28}$$

Further on, we assume $\varepsilon \ll 1$, so that the perturbations of the stationary core structure are weak. If the distance between defects is of order $O(\varepsilon^{-1})$, the defect velocity should be of order $O(\varepsilon)$. Therefore we rescale $\{\mathbf{U},\Omega\}\to\{\varepsilon\mathbf{U},\varepsilon\Omega\}$, $R\to R/\varepsilon$, and expand χ in the small parameter ε: $\chi = \chi_0 + \varepsilon\chi_1 + \ldots$. The zeroth-order function is $\chi_0 = \rho(r)\mathrm{e}^{\pm\mathrm{i}\,\phi}$, where $\rho(r)$ verifies eq. (10). The first-order equation can be written in a compact form [20]

$$\mathcal{H}(\chi_1,\overline{\chi}_1) = \mathcal{I}(\mathbf{r}), \tag{29}$$

containing the inhomogeneity

$$\mathcal{I}(\mathbf{r}) = (\mathbf{U}+\mathbf{u})\cdot\nabla\chi + \mathrm{i}\,(\Omega+\omega)\chi \tag{30}$$

and the linear operator

$$\mathcal{H}(\chi_1,\overline{\chi}_1) = \nabla^2\chi_1 + (1-2|\chi_0|^2)\chi_1 - \chi_0^2\overline{\chi}_1, \tag{31}$$

where the overline denotes the complex conjugate. This operator is self-conjugate, and has three eigenfunctions

$\varphi(r,\phi)$ with zero eigenvalue: the two vector components of $\nabla\chi_0 = \mathrm{e}^{\pm \mathrm{i}\,\phi}\mathbf{W}(r)$, where

$$\mathbf{W}(r) = \rho_r \left\{ \begin{array}{c} \cos\phi \\ \sin\phi \end{array} \right\} \pm \frac{\mathrm{i}\,\rho}{r} \left\{ \begin{array}{c} \sin\phi \\ -\cos\phi \end{array} \right\}, \qquad (32)$$

that correspond to the translational degrees of freedom in the plane, and the eigenfunction $\mathrm{i}\,\chi_0$ corresponding to the rotational degree of freedom.

The translation and rotation velocities are determined by the solvability condition of eq. (29), which requires the inhomogeneity to be orthogonal to the eigenfunctions with zero eigenvalue. To avoid far-field divergence, the solvability condition may be computed in a circle of radius L large compared to the core size but small on the far-field scale, *i.e.* $1 \ll L \ll \varepsilon^{-1}$. In this case, it has to be complemented by a contour integral over the bounding circle:

$$\mathrm{Re}\left\{ \int_0^L r\,\mathrm{d}r \int_0^{2\pi} \overline{\varphi}\,\mathcal{I}(r,\phi)\,\mathrm{d}\phi \right.$$
$$\left. + L\int_0^{2\pi} (\overline{\varphi}\partial_r\chi_1 - \chi_1\partial_r\overline{\varphi})_{r=L}\,\mathrm{d}\phi \right\} = 0. \qquad (33)$$

4.2 Area integrals

It follows from the symmetries of self-induced active and passive flow that the respective inhomogeneities do not project on the rotational eigenfunction $\mathrm{i}\,\chi_0$, and therefore the rotation Ω may be only caused by the vorticity of the external flow. We concentrate therefore on the translational eigenfunction. The only component of $\mathbf{u}$ yielding a non-vanishing contribution is the active self-induced flow term in a positive defect. Using eq. (27) to compute the respective component of the inhomogeneity in eq. (33) yields, after angular integration,

$$\int_0^L r\,\mathrm{d}r \int_0^{2\pi} \overline{\mathbf{W}} \left(\mathbf{u}_+^{(a)} \cdot \mathbf{W}\right) \mathrm{d}\phi =$$
$$\pi \int_0^L \mathrm{d}r \left\{ \begin{array}{c} \psi\rho_r^2 + r^{-1}\psi_r\rho^2 \\ -\mathrm{i}\,\rho\rho_r(r^{-1}\psi + \psi_r) \end{array} \right\}. \qquad (34)$$

Since the y-component of this vector expression is purely imaginary, the non-vanishing contribution comes only from the x-component, (directed along the "comet tail" of the defect). Although the angular dependence in eq. (23) has superficially the same structure, the contribution of a negative defect vanishes identically upon angular integration. Vanishing of the contribution of the passive flow is evident from the angular symmetry of eq. (27).

The contribution of the vorticity term $\mathrm{i}\,\omega\chi_0$ also comes only from the self-induced active flow in a positive defect, and here again only the x-component is real:

$$\mathrm{Re}\int_0^L r\,\mathrm{d}r \int_0^{2\pi} \mathrm{i}\,\overline{\mathbf{W}}\omega\rho\,\mathrm{d}\phi = -\pi\int_0^L \upsilon\rho^2\mathrm{d}r. \qquad (35)$$

Due to the 3-fold symmetry of the active flow in a negative defect, its contribution to the solvability condition always vanishes, as also does that of the passive flow.

It remains to compute the contribution of the translational term $\mathbf{U}\cdot\nabla\chi_0$:

$$\mathrm{Re}\int_0^L r\,\mathrm{d}r \int_0^{2\pi} \overline{\mathbf{W}}(r)\ (\mathbf{U}\cdot\mathbf{W}(r))\,\mathrm{d}\phi =$$
$$\pi\mathbf{U}\int_0^L \left(\frac{\rho^2}{r} + r\rho_r^2\right)\mathrm{d}r = \pi\mathbf{U}\ln\frac{L}{a_0} \qquad (36)$$

with $a_0 \approx 1.126$ computed using the numerical solution of eq. (10).

4.3 Computation at small β

We concentrate now on the active flow generated by a positive defect, which is the only source of self-propulsion. For a viscous layer with no vertical momentum transfer ($\beta = 0$), the obvious solution of eq. (18) is $\upsilon(r) = \rho(r) \asymp 1 - \frac{1}{2}r^{-2}$. In view of eq. (19), this leads to the far-field asymptotics $\psi(r) \asymp \frac{1}{3}r^2$, so that $\mathbf{u}^{(+)}$ diverges linearly in r at $r\to\infty$. If $\beta \ll 1$, viscous dissipation in passive layers is essential at $r \gg 1$ only, *i.e.* outside the defect core. Rescaling $r = s/\sqrt{\beta}$ and using the far-field asymptopics of $\rho(r)$ leads to the far-field equation

$$\upsilon_{ss} + s^{-1}\upsilon_s - (1+s^{-2})\upsilon + s^{-2} = 0. \qquad (37)$$

The solution satisfying the boundary condition $\upsilon(0) = 1$ and decaying at infinity is expressed in a standard way by

$$\upsilon(s) = K_1(s)\int \frac{I_1(s)}{s}\mathrm{d}s - I_1(s)\left[2\pi + \int \frac{K_1(s)}{s}\mathrm{d}s\right], \qquad (38)$$

where $I_j(x)$, $K_j(x)$ are modified Bessel functions. This solution approaches unity at $s\to 0$, thereby matching the outer asymptotics of the short-scale solution $\upsilon(r) = \rho(r) \asymp 1$ at $\beta = 0$. The leading term in the expansion of the integral in the second term evaluates to -2π, while the other terms decay exponentially. Therefore the divergence stemming from the asymptotic behaviour of the function $I_1(s)$ solving the homogeneous equation is compensated by adding 2π in the parenthesis. The resulting expression decays as s^{-2} or, in the original length units, as $1/(\beta r^2)$ at $r\to\infty$. The far-field solution is plotted in fig. 3.

The radial dependence of the stream function solving eq. (19) with the boundary condition $\psi(0) = 0$ and approaching a constant value at $r\to\infty$ is presented in the form

$$\psi(r) = \frac{1}{2}\left[r\int_r^\infty \upsilon(r')\mathrm{d}r' - \frac{1}{r}\int_0^r (r')^2\upsilon(r')\mathrm{d}r'\right], \qquad (39)$$

where $\upsilon(r) = \rho(r)$ in the core region and $\upsilon(r/\sqrt{\beta})$ is given by eq. (38) at $r \gg 1$. The crossover between the inner and outer expressions for $\upsilon(r)$ can be set using the next expansion terms: $\upsilon(r) = 1 - \frac{1}{2}r^{-2}$ in the outer limit of the inner solution and $\upsilon(r) = 1 - \frac{1}{8}\pi\sqrt{\beta}r$ in the inner

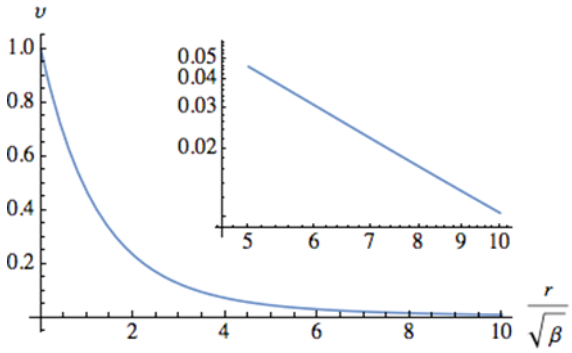

Fig. 3. The function $\upsilon(r)$ in the far field of a positive defect. Inset: logarithmic plot in the asymptotic region.

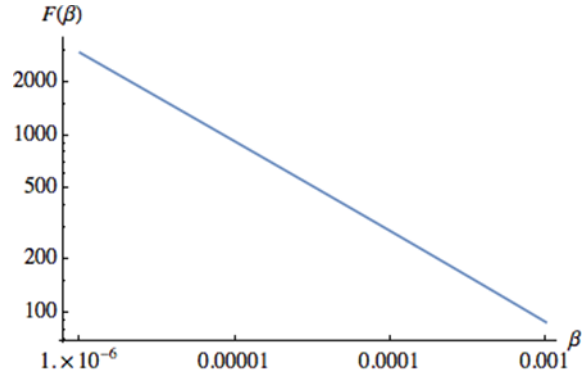

Fig. 4. The integral $F(\beta)$.

limit of the outer solution. the two expressions are equal at $r_0 = 2^{2/3}(\pi\sqrt{\beta})^{-1/3}$, which we choose as the crossover point. The derivative of $\psi(r)$ is

$$\psi_r = \frac{1}{2}\left[\int_r^\infty \upsilon(r')\mathrm{d}r' + \frac{1}{r^2}\int_0^r (r')^2\upsilon(r')\mathrm{d}r'\right] - r\upsilon(r). \tag{40}$$

Taking into account the asymptotics of $\upsilon(r) \sim r^{-2}$ at $r \to \infty$, we see that ψ_s indeed vanishes in this limit, since both the second integral and the last term decay as r^{-1}. The flow velocity can be subsequently obtained using eq. (27) but it is not required for evaluation of the solvability condition.

Taking into account the far-field asymptotics of $\upsilon(r), \psi(r)$ and $\rho(r)$, one can see that both integrals (34), (35) converge, decaying as L^{-1} at $L \gg 1$, so that the outer limit can be extended to infinity. Both integrals are evaluated separately in the core and far regions, taking into account the different length scales. Thus, eq. (35) is evaluated as

$$-\frac{\mathcal{I}_\omega}{\pi} = \int_0^{r_0} \rho^3(r)\mathrm{d}r + \frac{1}{\sqrt{\beta}}\int_{s_0}^\infty \upsilon(s)\mathrm{d}s, \tag{41}$$

where $s_0 = \sqrt{\beta}r_0 = (4/\pi)^{1/3}\beta^{1/6}$ and $\rho(r)$ is set to unity in the far region. In a similar way, eq. (34), is calculated separating the core and far regions and taking into account that in the latter the term $\psi\rho_r^2$ is negligible:

$$\frac{\mathcal{I}_\psi}{\pi} = \int_0^{r_0}\left[\psi\rho_r^2 + \frac{\psi_r\rho^2}{r}\right]\mathrm{d}r + \sqrt{\beta}\int_{s_0}^\infty \frac{\psi_s}{s}\mathrm{d}s. \tag{42}$$

This expression is most conveniently evaluated as a double integral using eqs. (39), (40). The sum $F(\beta) = -(\mathcal{I}_\omega + \mathcal{I}_\psi)/\pi$ is presented then as

$$F(\beta) = 2\int_0^{r_0}\rho^3(r)\mathrm{d}r + \frac{2}{\sqrt{\beta}}\int_{s_0}^\infty \upsilon(s)\mathrm{d}s - \frac{1}{2}\int_0^{r_0}\left[r\rho_r^2 + \frac{\rho^2}{r}\right]\mathrm{d}r\int_r^{r_0}\upsilon(r')\mathrm{d}r' + \frac{1}{2}\int_0^{r_0}\left[\frac{\rho_r^2}{r} - \frac{\rho^2}{r^3}\right]\mathrm{d}r\int_0^r (r')^2\upsilon(r')\mathrm{d}r' - \frac{1}{2}\sqrt{\beta}\int_s^\infty\frac{\mathrm{d}s'}{s'}\left[\int_{s_0}^\infty \upsilon(s)\mathrm{d}s + \frac{1}{s^2}\int_{s_0}^s (s')^2\upsilon(s')\mathrm{d}s'\right]. \tag{43}$$

We find that the second term is prevailing while the last one is negligible. The result is plotted in fig. 4. The dependence $F(\beta)$ is well approximated by a simple power law $F = \mathrm{e}/\sqrt{\beta}$.

5 Far-field solution

Unlike the integrals (34), (35), the area integral in eq. (36) diverges at $L \to \infty$, and therefore a cut-off is necessary. The respective contour integral dependent on the first-order solution χ_1 cannot be discarded but has to be evaluated by matching to the far-field solution. Assuming $L = O(\varepsilon^{-1/2})$, we have $\rho(L) = 1 - O(\varepsilon)$. It follows that the contour integral can be expressed, to the leading order $O(\varepsilon)$, through the phase field ϑ alone. The phase field, generally, evolves on a slow $O(\varepsilon^2)$ time scale and verifies the convection-diffusion equations obtained as the limiting form of the imaginary part of eq. (9):

$$\vartheta + \mathbf{u}\cdot\nabla\vartheta + \omega = \nabla^2\vartheta, \tag{44}$$

subject to the circulation condition $\oint \vartheta\,\mathrm{d}s = \pm 2\pi$ along any contour surrounding a single defect. The phase field determined by this equation depends both on advection by active or passive flow and phase gradients due to extant defects.

The problem has two small parameters, ε and β, and the relative strength of the above factors depends on their ratio. The active flow induced by a defect decays with the distance from its center as $\sqrt{\beta}/r$ (in the length units measured in ξ), while the phase gradient decays as ε/r. Thus, the action of the phase gradients prevails at $\sqrt{\beta}/\varepsilon \gg 1$, while advection dominates at $\sqrt{\beta}/\varepsilon \ll 1$. The former case is much more favourable for theory, since the variable velocity field, which itself depends on the phase field, makes the problem non-linear. The passive flow decays as $\zeta^{-1}(r/\varepsilon)^2$, and is not important in the case of well-separated defects, unless activity is very small. Assuming

a typical defect separation $R \sim \varepsilon^{-1}$, the passive flow is comparable with motion under the action of phase gradients at $\zeta \sim \varepsilon^2$.

The expressions for ϑ can be obtained in a simple form either for stationary defects or for defects propagating with a constant speed. In an active nematic layer containing a number of well-separated defects, one can distinguish between self-propulsion velocity of positive defects and velocity induced by the phase field of surrounding defects. The former is constant, up to slow rotation, which is estimated as $\Omega = O(\varepsilon^2)$, while the latter depends on a variable configuration of defects, and is likely to have zero average on a long time scale. It is reasonable therefore to compute the phase field assuming positive defects propagating with their self-propulsion velocity $\mathbf{U}$ and negative ones to be stationary. This approach is more reliable in the parametric domain $\varepsilon^2 \ll \beta \ll 1$ where the action of phase gradients dominates advection.

Neglecting advection, eq. (45) is rewritten in the frame comoving with a positive defect as

$$\mathbf{U} \cdot \nabla\vartheta + \nabla^2\vartheta = 0, \tag{45}$$

where the coordinates are extended by the factor ε and $\mathbf{U}$ is rescaled by the same factor. Since this equation is linear, the solution is a superposition of phase fields induced by all extant defects, $\vartheta = \sum \vartheta_i$. It is solved [25] by introducing a univalued function dual to ϑ, leading to a scale-invariant expression for the phase gradient:

$$\nabla\vartheta = \frac{1}{2}\,\mathrm{e}^{-(\mathbf{U}\cdot\mathbf{r})/2}\,\mathcal{J}\left[\mathbf{U}\,K_0\left(\frac{Ur}{2}\right) - \frac{U\mathbf{r}}{r}\,K_1\left(\frac{Ur}{2}\right)\right], \tag{46}$$

where $U = |\mathbf{U}|$, and $\mathcal{J}$ denotes clockwise rotation by the right angle. Taking the inner limit of eq. (46) at $r \to 0$, one can reconstitute the phase

$$\vartheta = \phi\frac{\mathbf{U}\times\mathbf{r}}{2}\ln\left(\frac{Ur}{4}e^{\gamma_\mathrm{E}-1}\right), \tag{47}$$

where $\gamma_\mathrm{E} \approx 0.577$ is the Euler constant. This expression can be used to determine the function χ_1 entering the contour integral:

$$\chi_1 = \mathrm{e}^{\mathrm{i}\,\vartheta} - \mathrm{e}^{\mathrm{i}\,\phi} = \mathrm{i}\,\mathrm{e}^{\mathrm{i}\,\phi}\frac{\mathbf{U}\times\mathbf{r}}{2}\ln\left(\frac{Ur}{4}e^{\gamma_\mathrm{E}-1}\right). \tag{48}$$

Using this in eq. (33), one can see that only its component along the x-axis has a non-vanishing real part, which is computed as

$$L\,\mathrm{Re}\int_0^{2\pi}(\partial_x\overline{\chi}_0\partial_r\chi_1 - \chi_1\partial_r\partial_x\overline{\chi}_0)_{r=L}\,\mathrm{d}\phi = \pi\mathbf{U}\ln\left(\frac{UL}{4}e^{\gamma_\mathrm{E}-1/2}\right). \tag{49}$$

When this contour integral is added to the area integral (36), the auxiliary radius L falls out. Adding also the integrals (34), (35) evaluated for $\beta \ll 1$ in sect. 4.3 and reverting to the original short-scale units, the solvability condition for a positive defect defining its self-induced velocity takes the form

$$\mathbf{U}\ln\frac{U_0}{\epsilon U} = -\varepsilon F(\beta)\widehat{\mathbf{x}}, \quad U_0 = \frac{4}{a_0}\mathrm{e}^{\gamma_\mathrm{E}-1/2} \approx 3.29, \tag{50}$$

where $\widehat{\mathbf{x}}$ is the unit vector along the x-axis, *i.e.* along the "comet tail" of the defect. Since, due to the small parameter in the denominator, the logarithm in the above formula is positive, and for tensile activity ($\zeta > 0$, hence $\varepsilon > 0$), the defect is pushed back from its tail.

For a stationary negative defect, the phase field solution is simply $\vartheta = -\phi$, and its dual is $\Phi = -\ln r$, so that $\chi_1 = 0$, and the self-induced phase field does not contribute to the contour integral. An additional contribution to the function χ_1 is due to the phase field gradient $\mathbf{A} = \sum \nabla\vartheta_i$ generated by other defects. This contribution varies in time as defects rearrange and is likely to be observed experimentally as a random jitter.

6 Discussion

Although the dynamics of defects is largely determined by active driving concentrated in the core of positive defects, the necessity of coupling inner and outer solutions makes the computations very complicated when a number of defects are present. Equation (50) has been derived under the assumption of rectilinear motion of positive defects, but, although their motion along the direction of the "comet tail" is prominent in experimental observations, both topological interactions and flow generated by other mobile defects lead to deviations from rectilinear trajectories. This random component of motion is similar in its origin to jitter of negative defects, and therefore statistics of motion of negative defects can be used to isolate the deterministic part of motion of positive defects and compare it with the prediction given by eq. (50).

Another source of experimental uncertainty lies in variations of the thickness of the interfacial active layer, which affects its effective viscosity η and activity ζ. Assuming that both parameters are proportional to the layer thickness, the dimensionless combination ε would be roughly constant but the other dimensionless parameter β will be variable. For both the above-mentioned reasons, the experimental data would contain a strong quasi-random component, and their reliable comparison to theoretical predictions would require compiling statistics of the velocity vectors of a large number of defects.

Author contribution statement

The authors have jointly planned the research and written the paper.

References

1. M.C. Marchetti, J.F. Joanny, S. Ramaswamy, T.B. Liverpool, J. Prost, M. Rao, R.A. Simha, Rev. Mod. Phys. **85**, 1143 (2013).

2. S. Ramaswamy, Annu. Rev. Condens. Matter Phys. **1**, 323 (2010).
3. A. Cavagna, A. Cimarelli, I. Giardina, G. Parisi, R. Santagati, F. Stefanini, M. Viale, Proc. Natl. Acad. Sci. U.S.A. **107**, 11865 (2010).
4. C. Dombrowski, L. Cisneros, S. Chatkaew, R.E. Goldstein, J.O. Kessler, Phys. Rev. Lett. **93**, 098103 (2004).
5. H.P. Zhang, A. Be'er, E.L. Florin, H.L. Swinney, Proc. Natl. Acad. Sci. U.S.A. **107**, 13626 (2010).
6. V. Schaller, C. Weber, C. Semmrich, E. Frey, A.R. Bausch, Nature **467**, 73 (2010).
7. Y. Sumino, K.H. Nagai, Y. Shitaka, D. Tanaka, K. Yoshikawa, H. Chate, K. Oiwa, Nature **483**, 448 (2012).
8. T. Sanchez, D.T. Chen, S.J. DeCamp, M. Heymann, Z. Dogic, Nature **491**, 431 (2012).
9. V. Narayan, S. Ramaswamy, N. Menon, Science **317**, 105 (2007).
10. A. Bricard, J.B. Caussin, N. Desreumaux, O. Dauchot, D. Bartolo, Nature **503**, 95 (2013).
11. S. Hernandez-Navarro, P. Tierno, J.A. Farrera, J. Ignes-Mullol, F. Sagues, Angew. Chem., Int. Ed. Engl. **53**, 10696 (2014).
12. W.F. Paxton, K.C. Kistler, C.C. Olmeda, A. Sen, S.K. St Angelo, Y. Cao, T.E. Mallouk, P.E. Lammert, V.H. Crespi, J. Am. Chem. Soc. **126**, 13424 (2004).
13. J. Howse, R. Jones, A. Ryan, T. Gough, R. Vafabakhsh, R. Golestanian, Phys. Rev. Lett. **99**, 048102 (2007).
14. J. Palacci, S. Sacanna, A.P. Steinberg, D.J. Pine, P.M. Chaikin, Science **339**, 936 (2013).
15. G. Henkin, S.J. DeCamp, D.T. Chen, T. Sanchez, Z. Dogic, Philos. Trans. A: Math. Phys. Eng. Sci. **372**, 0142 (2014).
16. P. Guillamat, J. Ignes-Mullol, F. Sagues, Proc. Natl. Acad. Sci. U.S.A. **113**, 5498 (2016).
17. P. Guillamat, J. Ignes-Mullol, S. Shankar, M. Marchetti, F. Sagues, Phys. Rev. E **94**, 060602(R) (2016).
18. F.C. Keber, E. Loiseau, T. Sanchez, S.J. DeCamp, L. Giomi, M.J. Bowick, M.C. Marchetti, Z. Dogic, A.R. Bausch, Science **345**, 1135 (2014).
19. P.G. de Gennes, J. Prost, *The Physics of Liquid Crystals* (Oxford University Press, Oxford, UK, 1993).
20. L.M. Pismen, *Vortices in Nonlinear Fields* (Clarendon Press, Oxford, 1999).
21. L.M. Pismen, Phys. Rev. E **88**, 050502(R) (2013).
22. L. Giomi, M.J. Bowick, X. Ma, M.C. Marchetti, Phys. Rev. Lett. **110**, 228101 (2013).
23. S.P. Thampi, R. Golestanian, J.M. Yeomans, Phys. Rev. Lett. **111**, 118101 (2013).
24. R.A. Simha, S. Ramaswamy, Phys. Rev. Lett. **89**, 058101 (2002).
25. E. Dubois-Violette, E. Guazelli, J. Prost, Philos. Mag. A **48**, 727 (1983).